ASIAN JOURNAL OF PHARMACEUTICAL AND CLINICAL RESEARCH

INNOVARE ACADEMIC SCIENCES
Knowledge to Innovation

Vol 18, Issue 12, 2025

Online - 2455-3891
Print - 0974-2441

Research Article

BIOMEDICAL APPLICATION OF SELENIUM NANOPARTICLES SYNTHESIZED USING *LINUM USITATISSIMUM* AND *WITHANIA SOMNIFERA* HERBAL FORMULATION

SURIYA M[1], KALAIMATHI J[1]*, REVATHI S[1], DEENA MOL J[1], KARTHIKA R[1], RAJESHKUMAR S[2], SURESH K[3]

[1]Department of Biochemistry, Theivanai Ammal College for Women (Autonomous), Affiliated to Annamalai University, Villupuram, Tamil Nadu, India. [2]Department of Anatomy, Centre for Global Health Research, Saveetha Medical College and Hospitals, Saveetha Institute of Medical and Technical Sciences, Chennai, Tamil Nadu, India. [3]Department of Biotechnology and Biochemistry, Annamalai University, Chennai, Tamil Nadu, India.

***Corresponding author: Kalaimathi J; Email: jkalaimathi1978@gmail.com**

Received: 25 July 2025, Revised and Accepted: 08 October 2025

ABSTRACT

Objectives: This study aimed to synthesize and characterize selenium nanoparticles (SeNPs) using phytochemical-rich extracts of *Linum usitatissimum* (flaxseed) and *Withania somnifera* (ashwagandha), and to evaluate their biological efficacy and safety for biomedical applications.

Methods: SeNPs were synthesized through a green method employing aqueous extracts of flaxseed and ashwagandha as reducing and stabilizing agents. Characterization was performed using ultraviolet (UV)-visible spectroscopy, X-ray diffraction (XRD), scanning electron microscopy, transmission electron microscopy (TEM), and Fourier transform infrared spectroscopy to determine morphology, crystallinity, and functional groups. Biological activities were assessed through antioxidant assays (2,2-diphenyl-1-picrylhydrazyl, Ferric reducing antioxidant power, ABTS), anti-inflammatory tests (bovine serum albumin and egg albumin denaturation), and antimicrobial evaluations (agar well-diffusion and time-kill assay). Cytotoxicity and embryonic toxicology were analyzed using brine shrimp lethality and zebrafish embryo viability assays.

Results: The UV-visible spectra confirmed nanoparticle formation with a characteristic peak at 270–280 nm. XRD and TEM analyses revealed crystalline SeNPs of ~25 nm stabilized by phytochemicals. SeNPs exhibited strong antioxidant activity (>75% inhibition), anti-inflammatory efficacy comparable to diclofenac sodium, and significant antimicrobial zones of inhibition at 100 µg/mL. Cytotoxicity was minimal at therapeutic doses, whereas zebrafish embryonic studies indicated dose-dependent toxicity at higher concentrations.

Conclusion: Green-synthesized SeNPs demonstrate potent antioxidant, anti-inflammatory, and antimicrobial properties, with good biocompatibility at therapeutic concentrations. Their eco-friendly synthesis and biological efficacy suggest strong potential as sustainable therapeutic agents, warranting further *in vivo* studies and clinical translation.

Keywords: Selenium nanoparticles, *Linum usitatissimum*, *Withania somnifera*, Green synthesis, Biomedical applications.

 DOI: http://dx.doi.org/10.22159/ajpcr.2025v18i12.56260. Journal homepage: https://innovareacademics.in/journals/index.php/ajpcr

INTRODUCTION

Nanotechnology has become a new revolution, providing new solutions in such areas as medicine, energy, and environmental science [1]. The promise of its potential is to manipulate matter at the nanoscale, and from that, materials are conferred with unique physical, chemical, and biological properties. In various aspects of nanotechnology advances, introducing nanoparticles in medicine has revolutionized diagnostics, the mode of drug delivery, and the forms of therapies. Due to their potential in solving various challenging issues in the field of health concerning their antioxidant, anti-inflammatory, and antimicrobial properties, selenium nanoparticles (SeNPs) have received enhanced interest [2,3]. Selenium is an important trace element crucial for sustaining one's health, mainly through playing a role in selenoproteins that prevent oxidative stress to cells and modulate the immune response [4].

Conventional selenium formulations, however, are faced by challenges such as poor bioavailability and toxicity at high doses [3]. The emergence of SeNPs represents a promising option, offering selenium the advantages of biocompatibility, stability, and therapeutic efficacy as well as integrating the benefits of selenium because of its nanoscale nature [5,6]. In recent years, attention has been fueled into green synthesis procedures for nanoparticle formation and termed eco-friendly and sustainable [7]. Such approaches employ such natural resources as plant extracts, acting as reducing and stabilizing agents, therefore, eliminating the need to use dangerous chemicals.

Of the two medicinal plants identified with a rich bioactive composition, flaxseed (*Linum usitatissimum*) and ashwagandha (*Withania somnifera*) are two of them [8]. These compounds not only catalyze the synthesis of SeNPs but also modify their biological properties to the advantage of making them excellent for biomedical applications [9]. Although research on the SeNPs has improved, there is still a gap in investigating the synergistic capability of these herbal extracts in nanoparticle synthesis [10]. Flaxseed and ashwagandha, which are rich in antioxidant and anti-inflammatory properties, provide a novel opportunity to produce biocompatible SeNPs customized for therapeutic uses [11]. With the bioactive compounds of these plants, it is possible to improve the stability as well as biocompatibility and efficacy of SeNPs, which are the limitations of conventional selenium formulations [12,13].

The purpose of this work is the synthesis of SeNPs with the use of *L. usitatissimum* and *W. somnifera* by the green synthesis method and evaluation for biomedical use. The data support the emerging area of so-called green nanotechnology and highlight the importance of plant-based synthesis options in the development of non-toxic functional and eco-friendly therapeutic agents.

METHODS

Preparation of plant extracts

For the preparation of plant extracts, 1 g of *W. somnifera* (ashwagandha) powder and 1 g of *L. usitatissimum* (flaxseed) powder were each suspended separately in 100 mL of distilled water, corresponding to a 1% (w/v) concentration. The mixtures were heated on a heating mantle at 60–70°C for 15–20 min to facilitate the extraction of bioactive compounds. After cooling to room temperature, the solutions were filtered using Whatman No. 1 filter paper to remove insoluble residues. The clear filtrates were collected and stored at 4°C until further use.

Formulation of the herbal extract mixture

To prepare the herbal formulation, equal volumes of the two extracts were combined in a 1:1 (v/v) ratio to ensure a balanced contribution of phytochemicals from both plants. This mixed extract served as the reducing and stabilizing agent for the green synthesis of SeNPs.

Synthesis of SeNPs

For SeNP synthesis, a 30 mM sodium selenite precursor solution was prepared in 50 mL of distilled water. To this, 50 mL of the herbal formulation (1:1 mixture of the 1% *W. somnifera* and *L. usitatissimum* extracts) was added dropwise under constant stirring at 600 rpm. The final reaction volume was therefore 100 mL. The reaction mixture was maintained at room temperature (25±2°C) for 24–48 h to allow the phytochemicals in the extracts to reduce and stabilize the selenium ions. The formation of SeNPs was monitored using a ultraviolet (UV)-visible spectrophotometer to detect the characteristic absorption peak (Fig. 1a-d).

Following synthesis, the suspension was centrifuged at 8,000 rpm for 10 min. The pellet containing SeNPs was washed twice with double-distilled water to remove unbound biomolecules and then air-dried. The purified SeNPs were stored in airtight Eppendorf tubes at 4°C until further characterization and biomedical application studies.

Characterization of SeNPs

The optical properties of the synthesized SeNPs were initially confirmed using a UV-visible spectrophotometer (UV-1800, Shimadzu, Japan) by recording the absorption spectra in the 200–800 nm range. The surface functional groups involved in the reduction and stabilization of nanoparticles were identified through Fourier transform infrared spectroscopy (FT-IR, Nicolet iS50, Thermo Fisher Scientific, USA) within the scanning range of 4,000–400 cm^{-1}. The crystalline nature and phase purity of the SeNPs were further examined by X-ray diffraction analysis (X'Pert PRO, PANalytical, Netherlands) using Cu Kα radiation (λ=1.5406 Å), and the average crystallite size was calculated employing the Debye–Scherrer equation. Morphological characteristics, including surface roughness and aggregation, were studied by scanning electron microscopy (SEM) (JSM-6390LV, JEOL Ltd., Japan), while particle size and lattice structure at the nanoscale were validated by high-resolution transmission electron microscopy (TEM) (JEM-2100, JEOL Ltd., Japan) operated at 200 kV.

Antimicrobial activity

Agar well diffusion technique

The antimicrobial activity of SeNPs synthesized using *L. usitatissimum* (flaxseed) and *W. somnifera* (ashwagandha) was evaluated using the agar well diffusion technique. Standard microbial strains, including *Escherichia coli*, *Staphylococcus aureus*, *Pseudomonas* spp., and *Candida albicans*, were used for the study. These strains were maintained on appropriate culture media, such as Mueller–Hinton agar for bacterial strains and Sabouraud dextrose agar for fungal strains. To prepare the microbial inoculum, active cultures were diluted in sterile saline to match the 0.5 McFarland turbidity standard, equivalent to approximately 1.5×1081.5\times 1081.5×108 colony-forming units (CFU/mL). The standardized inoculum was evenly spread onto the surface of solidified agar plates using a sterile swab to ensure uniform microbial growth.

A sterile polystyrene pipette tip was used to create 9 mm diameter wells in the inoculated agar plates. Each well was filled with 100 µL of SeNP suspensions prepared at concentrations of 25 µg/mL, 50 µg/mL, and 100 µg/mL. Standard antimicrobial agents, such as amoxyrite for bacterial strains and fluconazole for *C. albicans* were used for comparison. The plates were incubated under optimal conditions, with bacterial plates incubated at 37°C for 24 h and fungal plates incubated at 28°C for 48 h to allow adequate diffusion and microbial growth. Following incubation, the zones of inhibition around the wells were measured using a digital Vernier caliper to determine the antimicrobial efficacy of SeNPs.

Time kill curve assay

The time-kill curve assay was conducted to evaluate the antimicrobial efficacy of SeNPs synthesized using *L. usitatissimum* (flaxseed) and *W. somnifera* (ashwagandha) against selected microbial strains, including *E. coli*, *S. aureus*, *Pseudomonas* spp., and *C. albicans*. Freshly prepared cultures of the test organisms were standardized to a concentration of approximately 10^6 CFU/mL using sterile saline to ensure consistent inoculum across all samples. Aliquots of the microbial suspensions were treated with SeNP solutions at concentrations of 25 µg/mL, 50 µg/mL, and 100 µg/mL. Standards such as amoxyrite for bacteria and fluconazole for fungi and control (untreated samples) were included for comparison.

The treated and control samples were incubated at 37°C with gentle shaking to ensure uniform exposure and distribution. At specific time intervals (0, 1, 2, 3, 4, and 5 h), aliquots of 100 µL were withdrawn, and their optical density (OD) was measured at 600 nm using an enzyme-linked immunosorbent assay (ELISA) reader. This provided a quantitative measure of microbial growth or reduction over time.

Antioxidant activity

2,2-diphenyl-1-picrylhydrazyl (DPPH) assay

The antioxidant activity of SeNPs was assessed using the DPPH-free radical scavenging assay. DPPH, a stable-free radical, exhibits a violet color in methanol, which changes to yellow on reduction by an antioxidant. A stock solution of DPPH (0.1 mM) was prepared in methanol. The assay was performed by mixing 1 mL of DPPH solution with 1 mL of SeNPs at concentrations of 10, 20, 30, 40, and 50 µg/mL. The reaction mixtures were incubated in the dark at room temperature for 30 min to prevent photodegradation. After incubation, the absorbance was measured at 517 nm using a UV-visible spectrophotometer. Ascorbic acid (10–50 µg/mL) served as the standard antioxidant. The percentage of DPPH radical scavenging was calculated using the formula:

$$\text{Inhibition (\%)} = (\text{Acontrol} - \text{Asample}/\text{Acontrol}) \times 100$$

Hydrogen peroxide (H_2O_2 scavenging assay)

The SeNPs' ability to scavenge hydrogen peroxide was evaluated. A 40 mM H_2O_2 solution was prepared in phosphate buffer (pH 7.4). In a 1 mL reaction mixture, 0.6 mL of H_2O_2 solution was mixed with 0.4 mL of SeNPs at varying concentrations (10, 20, 30, 40, and 50 µg/mL). The solution was incubated for 10 min at room temperature. After incubation, the absorbance was measured at 230 nm using a UV-visible spectrophotometer. Ascorbic acid at similar concentrations was used as the standard. The percentage of H_2O_2 scavenging was calculated using the formula:

$$\text{Inhibition (\%)} = (\text{Acontrol} - \text{Asample}/\text{Acontrol}) \times 100$$

Ferric reducing antioxidant power (FRAP) assay

The reducing power of SeNPs was determined using the FRAP assay. The FRAP reagent was prepared by mixing 10 mM TPTZ (2,4,6-tripyridyl-s-triazine) solution in 40 mM HCl with 20 mM ferric chloride ($FeCl_3 \cdot 6H_2O$) and 300 mM acetate buffer (pH 3.6) in a 1:1:10 ratio. In a 1 mL reaction mixture, 0.3 mL of SeNPs at different concentrations (10, 20, 30, 40, and

50 µg/mL) was mixed with 0.7 mL of FRAP reagent. The mixture was incubated at 37°C for 30 min. The absorbance was measured at 593 nm. Ascorbic acid at equivalent concentrations was used as a standard. The results were expressed as the percentage increase in absorbance, reflecting the reducing power of the sample used,

Inhibition (%) = (Acontrol−Asample/Acontrol) × 100

ABTS assay

The antioxidant potential of SeNPs was also determined using the ABTS radical scavenging assay. ABTS radical cations were generated by mixing 7 mM ABTS with 2.45 mM potassium persulfate, followed by incubation in the dark at room temperature for 12–16 h. The ABTS solution was diluted with distilled water to obtain an absorbance of 0.7 at 734 nm. In a 1 mL reaction mixture, 0.3 mL of SeNPs at concentrations of 10, 20, 30, 40, and 50 µg/mL was mixed with 0.7 mL of ABTS solution. After 10 min of incubation in the dark, the absorbance was recorded at 734 nm. Ascorbic acid served as a reference standard, and the percentage inhibition of ABTS radicals was calculated using,

Inhibition (%) = (Acontrol−Asample/Acontrol) × 100

Nitric oxide scavenging assay

The nitric oxide scavenging activity of SeNPs was determined using sodium nitroprusside. Sodium nitroprusside (10 mM) in phosphate buffer (pH 7.4) was incubated with SeNPs at concentrations of 10, 20, 30, 40, and 50 µg/mL at 37°C for 2 h. After incubation, 0.5 mL of the reaction mixture was mixed with 0.5 mL of Griess reagent (1% sulfanilamide and 0.1% NEDD in 5% phosphoric acid). The absorbance of the pink chromophore formed was measured at 546 nm. Ascorbic acid was used as the standard. The percentage inhibition was calculated as:

Inhibition (%) = (Acontrol−Asample/Acontrol) × 100

Anti-inflammatory activity

Bovine serum albumin (BSA) denaturation assay

The inhibition of protein denaturation by SeNPs was studied using BSA. A reaction mixture containing 0.5 mL of 1% BSA solution, 0.5 mL of phosphate buffer (pH 6.3), and 0.5 mL of SeNPs (10–50 µg/mL) was incubated at 37°C for 20 min. The mixture was then heated at 70°C for 5 min to induce protein denaturation. After cooling, the absorbance was measured at 660 nm. Diclofenac sodium (10–50 µg/mL) was used as the standard. The percentage inhibition of protein denaturation was calculated as:

Inhibition (%) = (Acontrol−Asample/Acontrol) × 100

Egg albumin (EA) denaturation assay

A similar procedure was followed for the EA denaturation assay. EA (5% w/v) was prepared in distilled water. A 1 mL reaction mixture containing 0.5 mL of EA solution, 0.4 mL of phosphate buffer (pH 6.3), and 0.1 mL of SeNPs at varying concentrations (10–50 µg/mL) was heated at 70°C for 10 min. The mixture was cooled, and absorbance was recorded at 660 nm. Diclofenac sodium was used as the reference standard. The percentage inhibition was calculated using,

Inhibition (%) = (Acontrol−Asample/Acontrol) × 100

Membrane stabilization assay

The human red blood cell membrane stabilization method was used to assess anti-inflammatory activity. Blood samples were collected from healthy volunteers and centrifuged at 3000 rpm for 10 min to obtain RBCs, which were washed with isotonic saline. The RBC suspension was mixed with SeNPs (10–50 µg/mL) in a hypotonic solution. The mixture was incubated at 37°C for 30 min and centrifuged. The absorbance of the supernatant was measured at 540 nm. Diclofenac sodium was used as the standard. The percentage of hemolysis inhibition was calculated to evaluate membrane stabilization.

Inhibition (%) = (Acontrol−Asample/Acontrol) × 100

Cytotoxic effect

The cytotoxic effect of the SeNPs was evaluated using the Brine Shrimp Lethality Assay. For the preparation of saline water, 2 g of iodine-free salt was dissolved in 200 mL of distilled water. A 6-well ELISA plate was used, with each well filled with 10–12 mL of the saline solution and 10 brine shrimp nauplii. The SeNPs were added to each well at concentrations of 5, 10, 20, 40, and 80 µg/mL to assess their cytotoxicity. The plates were incubated for 24 h, after which the number of live nauplii was recorded. The percentage of mortality was calculated using the formula:

Mortality (%) = (Number of dead nauplii/Total number of nauplii) × 100.

This assay allowed for determining the cytotoxic concentration range of the nanoformulation on brine shrimp nauplii.

Zebrafish toxicology evaluation

Maintenance and breeding of zebrafish

Adult zebrafish (*Danio rerio*) were maintained in a recirculating water system under controlled laboratory conditions at 28 ± 2°C with a 14-h light/10-h dark cycle. The zebrafish were fed twice daily with commercial dry bloodworms to ensure optimal health. For breeding, male and female zebrafish were placed in a ratio of 2:1 in breeding tanks overnight. Fertilized embryos were collected within 4 h post-fertilization (hpf), the next morning, and rinsed using freshly prepared E3 medium (5 mM NaCl, 0.17 mM KCl, 0.33 mM $CaCl_2$, and 0.33 mM $MgSO_4$) to ensure cleanliness and viability.

Experimental setup

The test solutions were prepared by dispersing SeNPs in E3 medium at concentrations of 5, 10, 20, 40, 80 µg/mL. These solutions were sonicated for 15 min to ensure uniform dispersion and adjusted to a neutral pH (7.2–7.4). Zebrafish embryos were distributed into 12-well

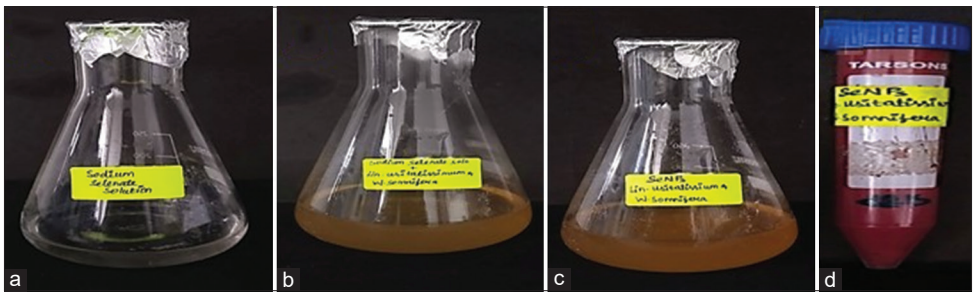

Fig. 1: Synthesis of selenium nanoparticles (SeNPs) using *Withania somnifera* and *Linum usitatissimum* plant extracts. (a) Sodium Selenite Solution (b) *W. somnifera* and *L. usitatissimum* Formulation (c) Green synthesized SeNPs solution (d) *Pellet of SeNPs L. usitatissimum and W. somnifera and Sodium selenate*

plates, with each well containing 2 mL of test solution and 20 embryos. A control group containing only E3 medium was maintained. Each concentration was tested in triplicate to ensure statistical reliability. The plates were incubated at 28 ± 1°C for 96 h, with deceased embryos removed every 12 h to prevent contamination. The plates were covered with aluminum foil to minimize light interference.

Observation and data collection

Embryos were observed at 24, 48, 72, and 96 h post-fertilization (hpf) using a stereomicroscope to monitor developmental stages, including cleavage, organogenesis, and hatching. The number of live and dead embryos was recorded at each interval, and viability rates were calculated. Morphological changes were documented, with special attention to abnormalities such as tail deformities, edema (pericardial or yolk sac), delayed hatching, and reduced pigmentation. Photographic documentation of normal and malformed embryos was performed using a Stereo microscope (COSLAB HL-10A) to provide visual evidence of developmental outcomes.

Statistical analysis

The data collected were expressed as mean ± standard deviation from three independent replicates. One-way analysis of variance followed by Tukey's *post hoc* test was used to compare the treated groups with the control. A $p<0.05$ was considered statistically significant, providing reliable insights into the toxicity and safety profile of the nanoparticles.

RESULTS

The UV-Visible absorption spectra (Fig. 2) of the green-synthesized SeNPs displayed a distinct surface plasmon resonance (SPR) band in the range of 270–280 nm, which is characteristic of nanoscale selenium. The spectra recorded at 36 and 48 h revealed stable and reproducible absorption patterns, with a gradual increase in absorbance intensity over time, confirming progressive nanoparticle formation and stabilization. A slight redshift was observed between the 2 time intervals, indicating growth and mild aggregation of particles during the synthesis process. The strong absorbance and stability of the band suggest effective reduction of selenium ions by the phytochemicals present in the *L. usitatissimum* and *W. somnifera* extracts, thereby validating successful nanoparticle synthesis.

FT-IR

The FTIR spectrum (Fig. 3) reveals the absorption bands which attest to the presence of different functional groups that have played a role in the reduction and stabilization of the SeNPs. Significant peaks were registered at 3405.6 cm^{-1}, which is the O-H stretching vibrations, and this warns of the presence of hydroxyl groups, whether from water or other biomolecules in the synthesis medium. The bands at 2921.1 cm^{-1} and 2852.4 cm^{-1} correspond to C-H stretching that suggests alkane groups. There were also additional peaks noted at 1647.5 cm^{-1} and 1547.5 cm^{-1}; C=C and C=O stretching vibrations, respectively, were highlighted. These peaks may correspond to the aromatic compound or carbonyl group, which may come from the organic stabilizers used in the greener synthesis medium. Vibrations at 1387.5 cm^{-1} and 1261.2 cm^{-1} are characteristic of C-N stretching vibrations and thus indicate the presence of amine groups. Finally, a well-defined peak at about 734.5 cm^{-1} matches Se-O bonds, thus proving the formation of SeNPs. The existence of these functional groups is an indication of proper capping and stabilization and which is a result of biocompatibility and stability of the synthesized SeNPs.

X-ray diffraction (XRD)

The diffractogram exhibits well-defined Bragg reflections characteristic of crystalline selenium (Fig. 4). Using the measured FWHM of the dominant reflection at $2\theta \approx 36°$ (Cu Kα, $\lambda = 1.5406$ Å; $K = 0.9$), Debye–Scherrer analysis gives a coherently diffracting domain size of ~1.9 nm. The peak positions match trigonal selenium referenced to JCPDS/ICDD card No. 06–0362, confirming the assigned phase. This nanometer-scale domain size is consistent with the ~5 nm primary particle diameter observed by TEM (domains ≤ particle size).

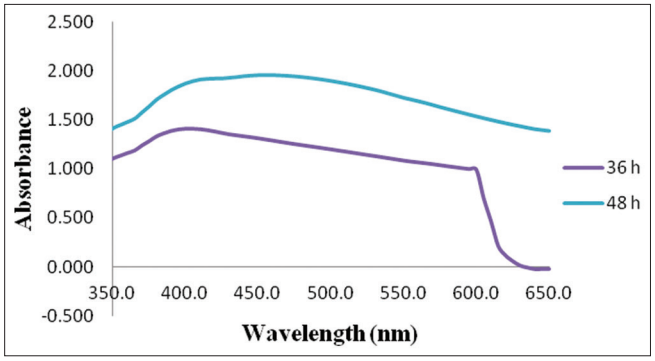

Fig. 2: Ultraviolet-visible spectroscopy analysis of selenium nanoparticles synthesized using *Withania somnifera* and *Linum usitatissimum* plant extracts

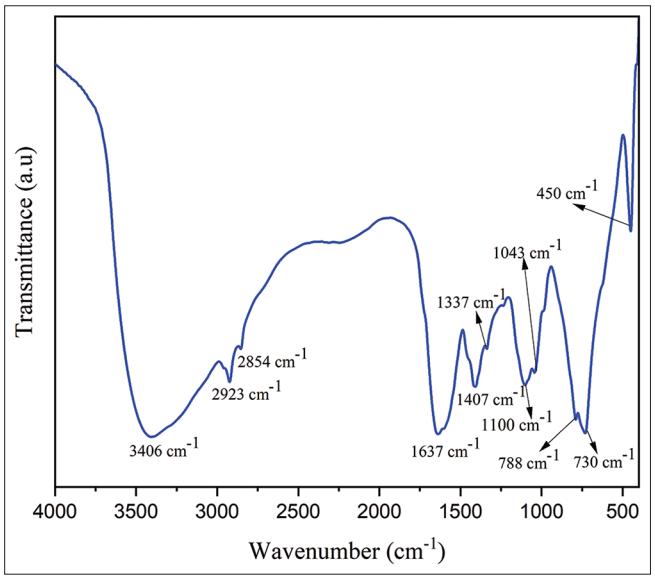

Fig. 3: Selenium nanoparticles (SeNPs) synthesized using *Withania somnifera* and *Linum usitatissimum* extracts, as confirmed by the Fourier transform infrared spectroscopy spectrum

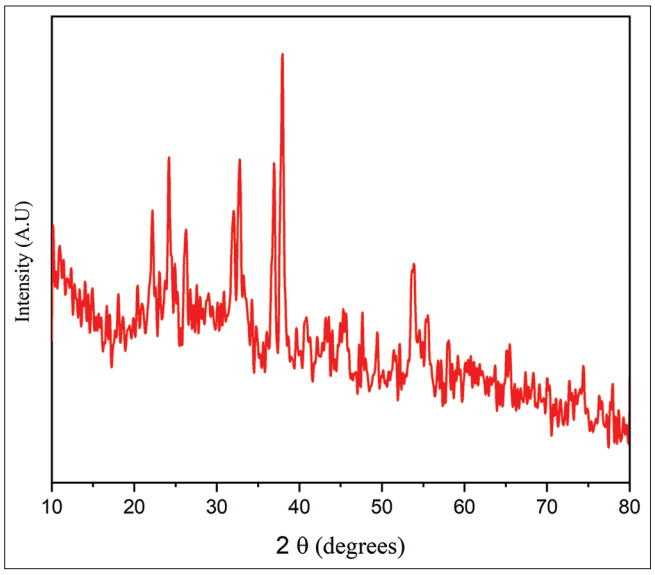

Fig. 4: Green-synthesized selenium nanoparticles using *Withania somnifera* and *Linum usitatissimum* extracts, confirmed by X-ray diffraction analysis

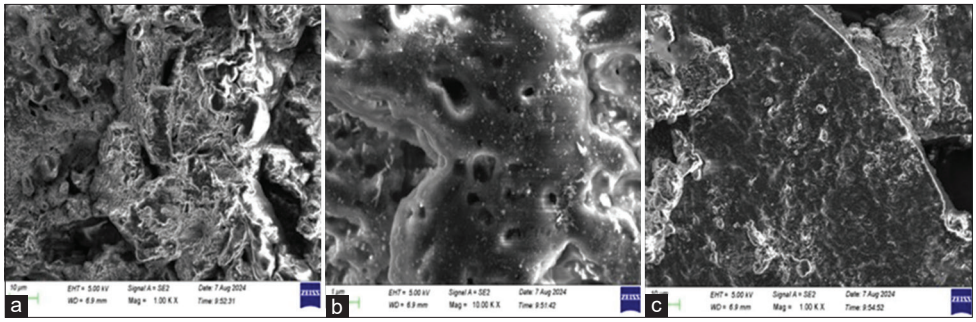

Fig. 5: Scanning electron microscopy images of selenium nanoparticles (SeNPs) synthesized using *Withania somnifera* and *Linum usitatissimum* extracts at different magnifications. (a) Aggregated SeNPs formed due to high surface energy, (b) Porous architecture providing a high surface area favorable for biomedical interactions, and (c) Detailed visualization of nanoparticle distribution showing rough and uneven surface texture that enhances functional properties

SEM

SEM micrographs (Fig. 5a-c) depict a hierarchically porous architecture composed of closely packed nanoscale subunits forming networked, rough-surfaced agglomerates. The surfaces appear corrugated with abundant interparticle voids, giving rise to ahigh-surface-area texture and extensive contact interfaces. This morphology is consistent across fields of view, indicating uniform synthesis and good reproducibility of the biogenic process. The micro-porosity and surface roughness observed are advantageous for biomedical use, as they can enhance adsorption, interfacial reactivity, and biomolecule interaction, thereby supporting the antioxidant, anti-inflammatory, and antimicrobial performance attributed to the SeNPs.

TEM

TEM micrographs (Fig. 6a and b) reveal discrete, nearly spherical SeNPs with well-resolved lattice fringes, confirming high crystallinity at the primary scale. High-resolution images (Fig. 6a; 5 nm scale bar) indicate a primary particle diameter of ~5 nm. Lower-magnification views (Fig. 6b; 500 nm scale bar) show these primaries arranged as sub-micron assemblies (typically ~100–500 nm) formed by gentle association during drying, while the ~5 nm cores remain clearly discernible. This hierarchical morphology crystalline ~5 nm primaries organized into larger, loosely packed clusters yields abundant interfacial area and accessible surface sites, attributes that are advantageous for biomolecular interactions and help rationalize the robust antioxidant, anti-inflammatory, and antimicrobial responses observed elsewhere in the study.

Antimicrobial activity

The antimicrobial potential of SeNPs, synthesized using *L. usitatissimum* and *W. somnifera*, was evaluated against *Pseudomonas* spp., *C. albicans*, *S. aureus*, and *E. coli* through the agar well-diffusion method. Three different concentrations of SeNPs – 25, 50, and 100 µg/mL were tested, and the inhibition zones were measured in millimeters to determine antimicrobial efficacy (Fig. 7a-d). At 25 µg/mL, SeNPs exhibited modest antimicrobial activity with inhibition zones of 8 mm for *Pseudomonas* spp., 7 mm for *C. albicans*, 11 mm for *S. aureus*, and 9 mm for *E. coli*. These findings suggest that even at lower concentrations, SeNPs can restrict microbial growth, with *S. aureus* being the most susceptible. As the concentration increased to 50 µg/mL, the inhibitory zones expanded-*Pseudomonas* spp. showed 10 mm, *C. albicans* 9 mm, *S. aureus* 15 mm, and *E. coli* 12 mm, indicating a dose-dependent enhancement in antimicrobial effect. The strongest activity was observed at 100 µg/mL, where inhibition zones reached 12 mm for *Pseudomonas* spp., 10 mm for *C. albicans*, 18 mm for *S. aureus*, and 14 mm for *E. coli*. Overall, *S. aureus* was the most sensitive organism, followed by *E. coli*, *Pseudomonas* spp., and *C. albicans*. Minimal or no zones of inhibition were observed in the control group, reinforcing the efficacy of SeNPs in suppressing microbial proliferation (Fig. 8).

Time kill curve assay

Concentration-dependent antimicrobial efficacy of synthesized SeNPs using *L. usitatissimum* and *W. somnifera* was studied using a time-kill curve assay against several microbial strains (Fig. 9). The respective number of SeNPs applied to bacterial strains (*Pseudomonas* spp., *S. aureus*, and *E. coli*) and *C. albicans* was 25, 50, and 100 µg/mL (with amoxyrite as the standard control). Bactericidal/fungicidal effects were studied by observing CFU/mL for 4 h. For *Pseudomonas* spp., SeNPs showed concentration-dependent reduction of CFU/mL over time. At 25 µg/mL, the subsequent CFU levels were still rather constant after an initial drop, which suggests a limited antimicrobial activity. On the other hand, there was a more pronounced decrease in CFU levels at 50 and 100 µg/mL; the 100 µg/mL concentration exhibited an effect close to amoxyrite at 4 h. This indicates that SeNPs at high concentration have significant bactericidal activity against *Pseudomonas* spp. For *C. albicans*, SeNPs also demonstrated concentration-dependent reduction in CFU/mL. Although there was a weak effect at the 25 µg/mL concentration, the cellular viability of fungi was significantly reduced at SeNPs concentrations of 50 µg/mL and 100 µg/mL. The inhibitory activity of SeNPs was consistent with the inhibitory activity of fluconazole at 100 µg/mL after 4 h, thus indicating that SeNPs can function as a good antifungal agent against *C. albicans* at greater concentrations.

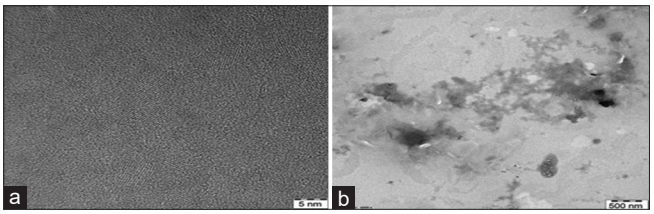

Fig. 6: Transmission electron microscopy images of selenium nanoparticles (SeNPs) synthesized using *Withania somnifera* and *Linum usitatissimum* extracts. (a) High-resolution image showing individual SeNPs with an average size of ~5 nm, confirming their nanoscale dimensions and crystalline nature; (b) aggregated SeNP clusters with size distribution up to ~500 nm, illustrating particle association and stabilization within the formulation

For *S. aureus,* all concentrations of SeNPs demonstrated a gradual decrease over time of CFU/mL, while 100 µg/mL concentrations had results that resembled those of amoxyrite. The 50 µg mL concentration also showed significant bactericidal activity, but it did not reach the efficacy point of the highest SeNP dose or the standard. Such findings suggest that SeNPs are actually capable of inhibiting *S. aureus* growth at relatively high concentrations. In *E. coli*, SeNPs exhibited concentration-dependent antimicrobial activity. The 25 µg/mL concentration had a slight decrease in CFU/mL, and the 50 µg/mL concentration had moderate bacterial inhibition. At 100 µg/mL, SeNPs had an extremely significant impact on bacterial viability, attaining an effect close to that brought about by amoxyrite at 4 h. This indicates that SeNPs possess high antibiotic functionalities towards *E. coli* when they are used at adequate numbers.

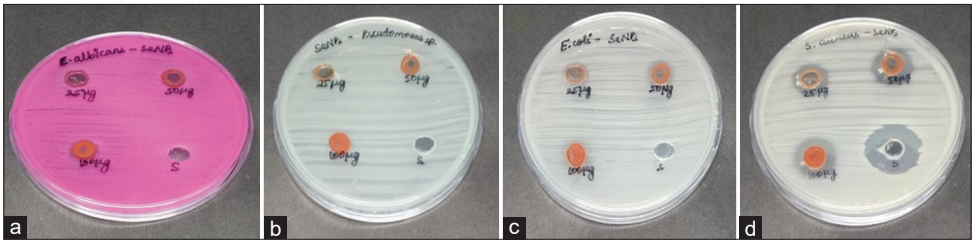

Fig. 7: Agar well-diffusion assay evaluating the antimicrobial activity of selenium nanoparticles (SeNPs) synthesized using *Withania somnifera* and *Linum usitatissimum* extracts. (a) *Candida albicans* with fluconazole as standard; (b) *Pseudomonas* spp. with amoxyrite as standard; (c) *Escherichia coli* with amoxyrite as standard; (d) *Staphylococcus aureus* with amoxyrite as standard. Zones of inhibition (measured in mm) demonstrate concentration-dependent antimicrobial effects of SeNPs

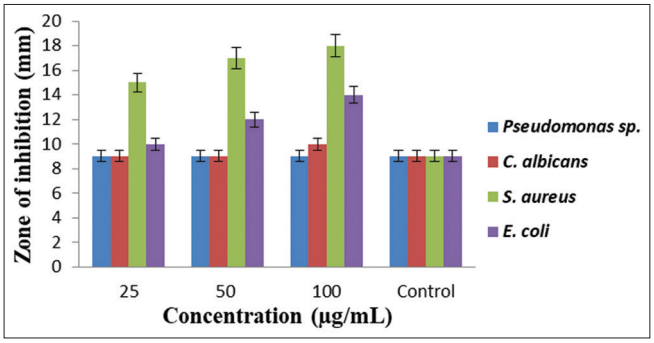

Fig. 8: Antimicrobial activity of selenium nanoparticles against *Staphylococcus aureus*, *Escherichia coli*, *Pseudomonas* spp., and *Candida albicans*. Data are presented as mean ± standard deviation (n=3). Statistical analysis was performed using one-way analysis of variance followed by Tukey's *post-hoc* test

Overall, the data reveal through the time-kill curve assay that the potent antimicrobial activity of SeNPs synthesized from *L. usitatissimum* and *W. somnifera* is effective across the strains of bacterial and fungal strains and is more pronounced at 100 µg/mL. Their effectiveness in decreasing microbial viability that comparable to amoxyrite and fluconazole, showing their possible use as antimicrobial agents in biomedical fields.

Anti-inflammatory activity

The *in vitro* anti-inflammatory activity of SeNPs was investigated using BSA denaturation, EA denaturation, and membrane stabilization assays with the formation of the anti-inflammatory formulation through *in vitro* synthesis of SeNPs using a herbal formulation of *L. usitatissimum* (flaxseed) and *W. somnifera* (ashwagandha). Diclofenac sodium was used as the standard anti-inflammatory agent, and SeNPs were assessed from 10 to 50 µg/mL concentrations. In the BSA denaturation assay, SeNPs demonstrated concentration-dependent enhancement of inhibition of protein denaturation. At 10 µg/mL, SeNPs exhibited approximately 50% inhibition, slightly lower than diclofenac sodium. At a 20 µg/mL concentration, inhibition grew to approximately 60%, indicating moderate efficacy. The inhibition rate was close to that of diclofenac sodium (about 65%) at 30 µg/mL. The inhibition rates by the higher concentrations of 40 and 50 µg/mL were 70% and above 75% respectively; comparable to the standard. These results indicate that SeNPs that were synthesized with an herbal formulation can inhibit the denaturation of protein, which is an indicator of the anti-inflammatory activity. The experimental results of the denaturation assay for EA also added to the anti-inflammatory activity of SeNPs. The minimum inhibition of around 55% was recorded by SeNPs at the lowest concentration of 10 µg/mL, which was comparable with that recorded for diclofenac sodium. At 20 µg/mL, this inhibition reached close to 60% suggesting increased activity. At 30 µg/mL, SeNPs showed about 65% inhibition and like diclofenac sodium and at 40 µg/mL inhibition rate increased to 70%. At the highest concentration, 50 µg/mL, the SeNPs showed more than 75% of inhibition, which was almost equal to the standard (Fig. 10).

Once more, SeNPs showed concentration-dependent activity in the membrane stabilization assay, which adds more evidence to their anti-inflammatory nature. Exposure to 10 µg/mL of SeNPs reveals a moderate membrane-stabilizing level of inhibition of about 55%. Ratios of inhibition improved in parallel with increased concentration, reaching 60% and 65% at 20 µg/mL and 30 µg/mL, respectively, closely following the results for diclofenac sodium. For high concentrations of 40 and 50 µg/mL, SeNPs showed inhibition levels of ca. 70% and almost 75%, respectively, and comparable with the standard. The membrane stabilization activity of SeNPs suggests their capacity to prevent cell membranes from destabilization, critically important for minimizing inflammation with lysosomal enzyme release. In general, these anti-inflammatory assays show that SeNPs synthesized with *L. usitatissimum and W. somnifera* have high anti-inflammatory activity on all the tested concentrations - similar to diclofenac sodium.

Antioxidant activity

The antioxidant potential of SeNPs synthesized using a herbal formulation of *L. usitatissimum* (flaxseed) and *W. somnifera* (ashwagandha) was comprehensively investigated with DPPH, H_2O_2 scavenging, FRAP, ABTS, and nitric oxide scavenging assays (Fig. 11). These assays determined the capacity of the SeNPs to neutralize-free radicals and the oxidation of reagents over concentrations of 10–50 µg/mL and compared to the results from a standard antioxidant. SeNPs had significant concentration-dependent extravasation of radical scavenging activity in the DPPH assay. With 70% inhibition, SeNPs tackled this at 10 µg/mL, and as the increase in concentration increased up to 20 and 30 µg/mL, the rates of inhibition bore about 75% and 80%, approximating well with the standard antioxidant. Increased 40 and 50 µg/mL concentrations provided inhibition levels of 82% and 85%, respectively, indicating the high level of free radical scavenging ability of SeNPs at elevated doses. None of this low activity is suggestive that SeNPs formed with herbal extracts exhibit high levels of antioxidant properties, which may be useful for biomedical purposes in oxidative stress. The hydrogen peroxide scavenging assay also found the antioxidant activity of SeNPs enhanced with concentration. At the lowest concentration, 10 µg/mL, medium inhibition of about 50% was observed for SeNPs. This activity rose to 60% at 20 µg/mL and 65% at 30 µg/mL. At high concentrations of 40 and 50 µg/mL, SeNPs effected inhibition at levels close to around 70% and 80%, respectively, on par with that of the standard. The resultant findings imply that SeNPs can neutralize hydrogen peroxide, which is a common reactive oxygen species, especially at high concentrations.

In FRAP, SeNPs showed consistent significant reducing activity at all used concentrations. At 10 µg/mL, SeNPs exhibited ca. 75% inhibition, which revealed high electron-donating activity even when administered at lower doses. This effect increased ever so slightly with increased concentrations, where inhibition rates of ~77% were found at 20 µg/mL, 80% at 30 µg/mL, and 82% at 40 µg/mL. The highest SeNPs concentration used (50 µg/mL) showed almost 90% inhibition, similar to the standard antioxidant. This highly reducing nature helps in the possible application of SeNPs as antioxidants, with their values added in therapeutic use. ABTS radical scavenging assay showed pure potency of SeNPs in all test concentrations.

At 10 µg/mL, the inhibition rate for SeNPs was approximately 75% and was closely comparable with the standard. Inhibition rate was slightly increased by concentration - approximately 78% at the concentration of 20 µg/mL, 80% at the concentration of 30 µg/mL, and 82% at the concentration of 40 µg/mL. At 50 µg/mL, SeNPs showed more than 85% inhibition, thereby indicating that they have significant antioxidant strength. This strong ABTS scavenging capability indicates that SeNPs synthesized with *L. usitatissimum* and *W. somnifera* has a great ability in minimizing oxidative damage, thus appropriate for biomedical applications for oxidative stress reduction.

The nitric oxide (NO) scavenging assay also revealed the antioxidant potential of SeNPs, with high inhibition rates in all the concentrations. At 10 µg/mL, SeNPs exhibited about 75% inhibition, indicating that NO scavenging activity was even more pronounced at a lowered concentration. This inhibition was constant with increasing concentrations, attaining approximately 77% at 20 µg/ml, about 78% at 30 µg/ml, and 80% at 40 µg/ml. At 50 µg/mL, the inhibition rate was closely approximated at about 85% and the standard antioxidant. NO scavenging performance is of special relevance in biomedical applications since nitric oxide radicals are linked to inflammatory and oxidative damage.

Cytotoxic effect

The cytotoxic effect of SeNPs was evaluated using a brine shrimp lethality assay, assessing the percentage of live nauplii over 2 days at varying SeNP concentrations (5, 10, 20, 40, and 80 µg/mL), with a control group for comparison. As shown in Fig. 12, the viability of nauplii remained above 80% across all tested concentrations, indicating minimal cytotoxicity of SeNPs at the examined doses.

On Day 1, all SeNP concentrations demonstrated high viability rates, ranging from approximately 95% to 100%, with no significant decrease in nauplii survival compared to the control. On Day 2, a modest decline in viability was noted, especially at the elevated concentrations of 40 and 80 µg/mL; however, survival rates of the nauplii stayed consistently above 85% across all test groups. This minimal decline suggests a concentration-dependent but low cytotoxic effect of SeNPs over an extended exposure period.

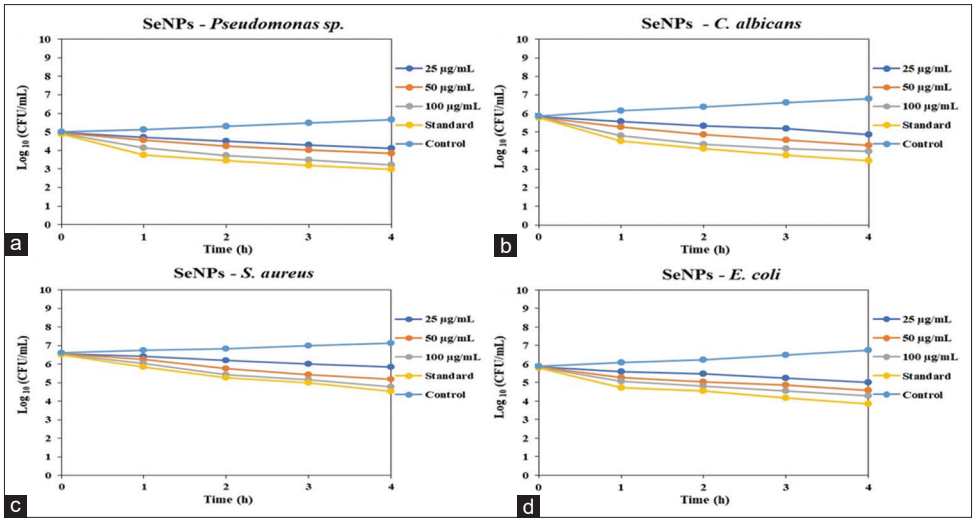

Fig. 9: Time-kill curve assay of green-synthesized selenium nanoparticles. (a) *Pseudomonas* spp. with amoxyrite as standard; (b) *Candida albicans* with fluconazole as standard; (c) *Staphylococcus aureus* with amoxyrite as standard; (d) *Escherichia coli* with amoxyrite as standard. Results expressed as mean ± standard deviation (n=3). One-way analysis of variance with Tukey's *post-hoc* test confirmed significance of dose- and time-dependent effects

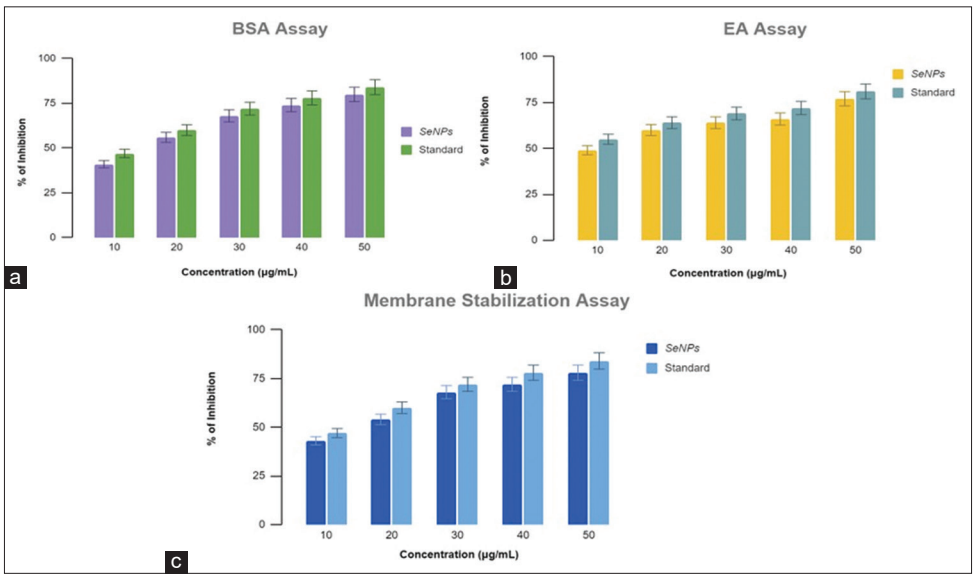

Fig. 10: Green-synthesized selenium nanoparticles tested for anti-inflammatory effects. (a) Bovine serum albumin denaturation assay (b) Egg albumin Denaturation assay (c) Membrane stabilization assay

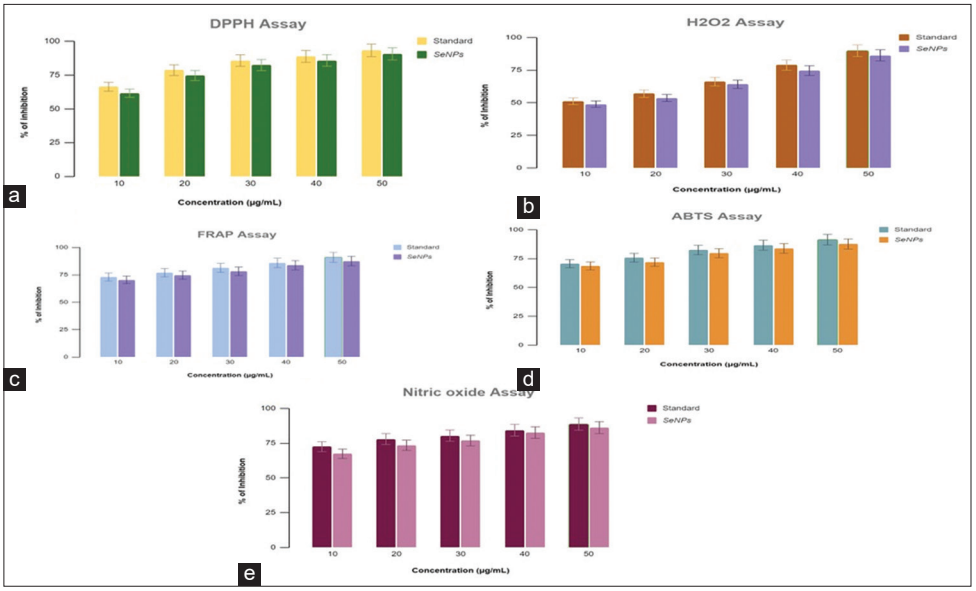

Fig. 11: Antioxidant activity of selenium nanoparticles measured using 2,2-diphenyl-1-picrylhydrazyl, H_2O_2 scavenging, Ferric reducing antioxidant power, ABTS, and nitric oxide assays. Data expressed as mean ± standard deviation (n=3). Statistical comparisons with standards were analyzed using one-way analysis of variance with Tukey's *post-hoc* test

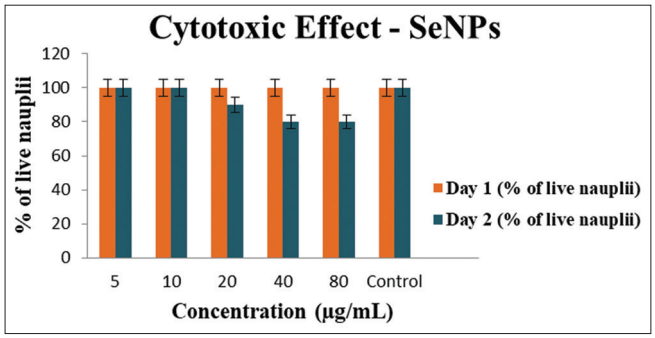

Fig. 12: Brine shrimp lethality assay showing the percentage viability of nauplii exposed to varying concentrations of selenium nanoparticles (5–80 µg/mL). Data expressed as mean ± standard deviation (n=3). Statistical analysis performed using one-way analysis of variance

The results indicate that SeNPs exhibit low cytotoxicity toward nauplii at the tested concentrations, suggesting their potential biocompatibility and safety for applications that may require prolonged exposure to SeNPs.

Embryonic toxicology

Fig. 13, Hatching rate of zebrafish embryos exposed to selenium nanoparticles at different concentrations (5–80 µg/mL). Embryonic toxicity of SeNPs was evaluated by monitoring the hatching rates of nauplii exposed to varying concentrations of SeNPs (5, 10, 20, 40, and 80 µg/mL), with comparisons made against an untreated control group. As shown in Fig. 14, a concentration-dependent decrease in hatching rate was noted, which may presage exposure to the toxic effects of high concentrations of SeNPs. In the control group, the hatching rate was almost 100% indicating a satisfactory embryonic development in the absence of SeNP exposure. Even at the lowest concentration of 5 µg/mL, the hatching rates were high and close to the control, indicating a negligible toxic effect at this level.

Nonetheless, there was a marked decline in hatching rate when the concentration was raised. In particular, at 40 µg/mL and 80 µg/mL, the hatching rate plummeted by about 55% and 40% correspondingly. These results indicate that higher concentration levels of SeNPs can impede the development of the embryo, as shown in hatching rates, at high levels of doses.

The viability rate of zebrafish embryos was assessed after exposure to varying concentrations of SeNPs, specifically at 5, 10, 20, 40, and 80 µg/mL, with a control group for comparison. As shown in Fig. 15, a concentration-dependent decline in viability was observed, indicating potential toxicity at higher concentrations of SeNPs.

The control group exhibited nearly complete viability, with survival rates approaching 100%, confirming ideal embryonic development in the absence of SeNP exposure. At the lowest concentration of 5 µg/mL, the viability rate remained comparable to the control, suggesting minimal toxic effects at this dose. However, with increasing concentrations, a gradual reduction in viability was evident. Notably, at concentrations of 40 µg/mL and 80 µg/mL, the viability rate significantly decreased to approximately 70% and 60%, respectively.

These results suggest that SeNPs exert a concentration-dependent toxic effect on zebrafish embryos, with higher concentrations leading to a noticeable decline in viability

DISCUSSION

L. Usitatissimum and *W. somnifera* herbal formulation was explored for the synthesis, characterization, and biomedical applications of SeNPs. The findings emphasize the applicability of these biogenic SeNPs for diverse therapeutic and environmental applications and their efficiency, safety, and functional diversity. Bioactive compounds obtained from flaxseed and ashwagandha were used in the bio-green synthesis method to inhibit selenium precursors and to stabilize nanoparticles formed. This environmentally friendly technique removes the necessity to use toxic chemicals and increases SeNPs [14,15] biocompatibility.

The results of UV-visible spectroscopy confirmed successful synthesis; the characteristic SPR peak at 270–280 nm documents the nanoscale size of the synthesized particles. Over time, the expected absorption increment and mild redshift indicated ongoing particle generation and stabilization; this was likely influenced by the extended reduction process and surface functionalization by herbal phytochemicals [16,17]. Not only did the presence of the bioactive compounds, such as polyphenols and flavonoids, in reduction and stabilization processes

Fig. 13: Hatching rate of zebrafish embryos exposed to selenium nanoparticles at different concentrations (5–80 μg/mL). Data expressed as mean ± standard deviation (n=3). Statistical analysis confirmed significant concentration-dependent differences

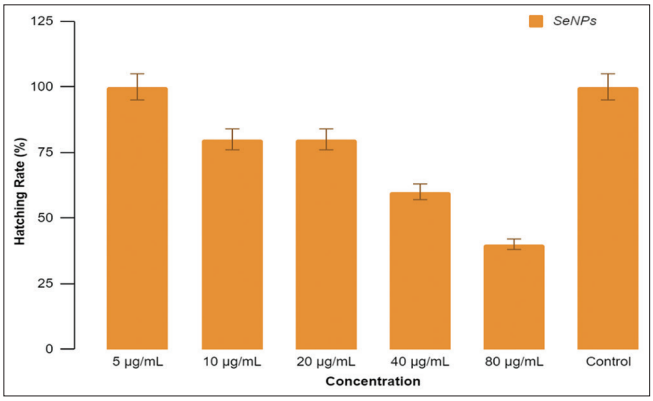

Fig. 14: Hatching Rate of Zebrafish Embryos Exposed to selenium nanoparticles. Results expressed as mean ± standard deviation (n=3). Statistical analysis performed using one-way analysis of variance with Tukey's *post-hoc* test

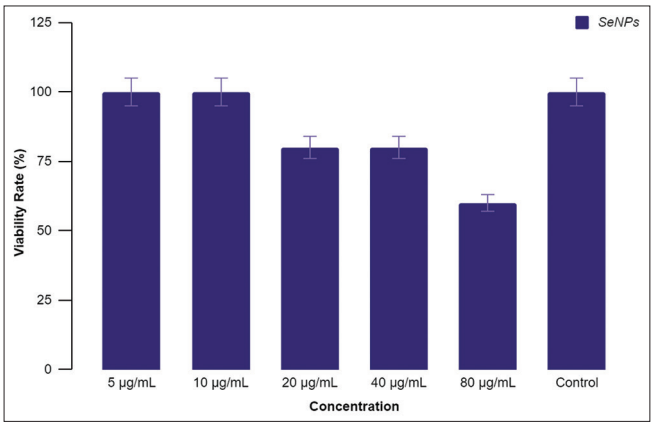

Fig. 15: Viability (%) of zebrafish embryos exposed to different concentrations of selenium nanoparticles (5–80 μg/mL). Results expressed as mean ± standard deviation (n=3). Statistical analysis performed using one-way analysis of variance with Tukey's *post-hoc* test

enable the controlled particle formation, but they also provided functional groups that increased the biological activity of the nanoparticles. These functionalized nanoparticles proved to be stable over a long time period for which it was suitable for biomedical uses that require prolonged efficacy [18,19].

Extensive characterization with SEM, TEM, XRD, and FTIR methods provided key information regarding the nature, size, composition, and surface chemistry of the synthesized SeNPs. SEM analysis revealed the porous character and an aggregated state of the nanoparticles, which suggests a high surface energy [18,20]. TEM images agreed with the existence of the spherical morphology and nanoscale dimensions (50–80 nm) of SeNPs with well-defined crystalline lattices supported by XRD. Obviously, the crystalline structure having an average crystallite size of ~25 nm is very important for the improvement of stability, optical properties, and reactivity, therefore making these nanoparticles suitable for a wide range of applications [21,22].

FTIR has determined the presence of functional groups (-OH), (-C=O), (-NH_2), and (Se-O) that assisted in stabilization and biological interactions. These functional groups helped to increase colloidal stability and biocompatibility and provide reactive sites for additional functionalization. The consistency of sizes, crystalline form, and functionalized surfaces is emphasized in the appropriateness of these SeNPs for therapeutic and diagnostic uses [23,24]. The use of SeNPs demonstrated defined antimicrobial potency against a large array of bacterial and fungal agents such as *Pseudomonas* spp., *S. aureus*, *E. coli,* and *C. albicans*. The microbial growth inhibition that is dose-dependent was confirmed in terms of time-kill assay experiments and the agar well-diffusion tests [1]. SeNPs at higher concentrations (100 μg/mL) showed effects similar to standard microbial agents such as amoxyrite and fluconazole, thus indicating their substitution potential in replacing the traditional antibiotics [25,26]. The base of the antimicrobial activity is ROS (reactive oxygen species) generation, microbial membrane permeation, and interference with some metabolic processes as ATP synthesis [27]. The particle size reduction and high surface-to-volume ratio improved nanoparticle interaction with microbial cells, which accounted for its bactericidal and fungicidal nature. The capability of SeNPs to inhibit biofilm formation is most promising in dealing with chronic infections that come with biofilm-associated pathogens [20].

The anti-inflammatory nature of SeNPs was shown through BSA denaturation, EA denaturation, and membrane stabilization assays. The nanoparticles had proven inhibition of protein denaturation and stabilization of lysosomal membranes, while effects were similar at higher concentrations [3]. These findings imply that SeNPs are capable of successfully modulating inflammatory pathways by preventing protein unfolding and membrane destabilization – key pathways into inflammation [28]. The joint effect of selenium and the phytochemicals in the herbal formulations strengthens this anti-inflammatory potential of SeNPs. These compounds presumably mediated the action of pro-inflammatory cytokines and decreased oxidative stress, thereby increasing the therapeutic efficacy of the nanoparticle [13,29]. SeNPs showed strong antioxidant activity in all assays (DPPH, FRAP, ABTS, and nitric oxide scavenging). The increase in radical scavenging and reducing power, which is dependent on concentration, in turn underscores the effectual nature of the compound in the neutralization of oxidative stress, which is one of the major initiators of chronic diseases, including cancer, cardiovascular disorders, and neurodegeneration [20,30]. Antioxidant potential of Se NPs is attributed to their nanoscale size, which enhances reactivity of its surface and the bioactive compounds from flaxseed and ashwagandha added to give additional radical-scavenging capabilities [5]. The capacity of SeNPs to attenuate oxidative stress makes them good potential fibers for antioxidative treatment.

In comparison to traditional antioxidants, SeNPs provide enhanced bioavailability and cellular uptake, being functionalized with surfaces and in the nanoscale [31].

Cytotoxicity testing through brine shrimp lethality assays indicated very low toxicity at lower concentrations, wherein viability was greater than 80% at higher dosages (80 µg/mL). Nevertheless, the zebrafish embryo viability test demonstrated a concentration-dependent decrease in survival and hatching rate, with toxicity noted at concentrations above 40 µg/mL. The results are indicative that while SeNPs are biocompatible at therapeutic doses, their possible toxicity at higher concentrations should be properly optimized in order to provide safe application [3,32]. Embryonic toxicology that is observed signifies the need for balance between efficacy and safety. Limited use of SeNPs can be reported in drug delivery and antimicrobial applications, where low concentrations support the viability of its application, while higher doses may cause oxidative stress and developmental disturbances requiring attention to dosage control in both categories (biomedical and environmental) of application [28,33].

Applications and future perspectives

This research study presents the wide potential of SeNPs for biomedical applications such as drug delivery, antioxidative therapeutics, and anti-microbial cures. Their low toxicity when used at therapeutic concentrations, combined with their solid therapeutic utility, makes them promising alternatives to the conventional agents. In addition, they can inhibit biofilm formation and regulate oxidative stress, enhancing their utility therapeutically in controlling chronic infectious disease and inflammation-related disorders [34]. SeNPs also have special properties that find beneficial use in environmental applications, for example, antimicrobial coatings and water purification. Nevertheless, the possibilities of the impact on the ecology of high-dose exposure require additional risk assessment for their proper use in the aquatic environment [6]. Further studies are expected to be concerned with tuning of synthesis parameters to obtain uniform size and increased stability, but with reduced toxicity. The utilization of targeting ligands or protective agents as functionalization may enable further development of the therapeutic potential of SeNPs. *In vivo* studies are essential for confirming their efficacy, pharmacokinetics, and safety profiles, which lead them back to clinical and industrial uses [35].

CONCLUSION

This study successfully formulated SeNPs from *L. usitatissimum* (flaxseed) and *W. somnifer*a (ashwagandha) by an environmentally friendly green synthesis. Their nanoscale dimensions, stability, and utility were supported by an extensive characterization. Analytical tools such as UV-visible spectroscopy, XRD, FTIR, SEM, and TEM revealed the structural integrity of the nanoparticles, surface functionalization, and crystalline nature. The major findings of the biomedical examination were strong antioxidant, anti-inflammatory, and antimicrobial traits. The SeNPs exhibited strong radical scavenging activity and membrane stabilization effects, and thus are valuable candidates for the management of oxidative stress and inflammation. Their broad-spectrum antimicrobial efficacy remains the key moot point as they have the potential to be alternatives to the existing class of antibiotics, particularly for confronting drug-resistant pathogens. Toxicological investigations suggested minimum cytotoxicity at therapeutic concentrations; however, the dose-dependent embryonic toxicity at higher concentrations limits the application and emphasizes the need for critical optimization of dosage for safe usage. A combination of selenium and phytochemicals contributed to effective biological activities of SeNPs without compromising eco-compatibility. Overall, in this study, the synthesized biogenic SeNPs possess enormous potential for biomedical and environmental applications. Further research should be concerned with *in vivo* validation, optimization of synthesis parameters, and functionalization approaches, to optimize efficacy and safety, and lay the ground for their clinical and industrial translation.

ACKNOWLEDGMENTS

The authors would like to express their sincere gratitude to the Research Supervisor, Department of Biochemistry, Theivanai Ammal College for Women (Autonomous), Villupuram, for her invaluable guidance, encouragement, and expertise throughout the study. Special appreciation is also extended to the research team at Saveetha Medical College, Chennai, and Annamalai University, Chidambaram, for their collaborative support and technical assistance.

AUTHORS CONTRIBUTIONS

MS conducted the laboratory experiments, collected the data, and drafted the manuscript. SR, DM, and RK were responsible for the investigation, methodology optimization, and statistical analysis. JK, SRK, and KS contributed to the study design, coordination, and manuscript revision. All authors read and approved the final version of the manuscript.

CONFLICT OF INTEREST

The Authors declare no conflict of interest.

FUNDING

Nil.

ETHICAL ISSUES

None.

REFERENCES

1. Hernández-Díaz JA, Garza-García JJ, León-Morales JM, Zamudio-Ojeda A, Arratia-Quijada J, Velázquez-Juárez G, *et al*. Antibacterial activity of biosynthesized selenium nanoparticles using extracts of *Calendula officinalis* against potentially clinical bacterial strains. Molecules. 2021 Sep 30;26(19):5929. doi: 10.3390/molecules26195929, PMID 34641478
2. Khudier MA, Hammadi HA, Atyia HT, Al-Karagoly H, Albukhaty S, Sulaiman GM, *et al*. Antibacterial activity of green synthesized selenium nanoparticles using *Vaccinium arctostaphylos* (L.) fruit extract. Cogent Food Agric. 2023 Dec 31;9(1):2245612. doi: 10.1080/23311932.2023.2245612
3. Muhammed RA, Mohammed S, Visht S, Yassen AO. A review on development of colon targeted drug delivery system. Int J Appl Pharm. 2024;16(2):12-27. doi: 10.22159/ijap.2024v16i2.49293
4. Nagalingam M, Rajeshkumar S, Balu SK, Tharani M, Arunachalam K. Anticancer and antioxidant activity of *Morinda citrifolia* leaf mediated selenium nanoparticles. J Nanomater. 2022;2022(1):2155772. doi: 10.1155/2022/2155772
5. Sentkowska A, Pyrzyńska K. The influence of synthesis conditions on the antioxidant activity of selenium nanoparticles. Molecules. 2022 Apr 12;27(8):2486. doi: 10.3390/molecules27082486, PMID 35458683
6. Tendenedzai JT, Chirwa EM, Brink HG. Harnessing selenium nanoparticles (SeNPs) for enhancing growth and germination, and mitigating oxidative stress in *Pisum sativum* L. Sci Rep. 2023 Nov 21;13(1):20379. doi: 10.1038/s41598-023-47616-5, PMID 37989844
7. Nath D, Kaur L, Sohal HS, Malhi DS, Garg S, Thakur D. Application of selenium nanoparticles in localized drug targeting for cancer therapy. Anti-Cancer Agents Med Chem. 2022 Aug 4;22(15):2715-25. doi: 10.2174/1871520622666220215122756, PMID 35168523
8. Xia Y, Chen Y, Hua L, Zhao M, Xu T, Wang C, *et al*. Functionalized selenium nanoparticles for targeted delivery of doxorubicin to improve non-small-cell lung cancer therapy. Int J Nanomedicine. 2018 Oct 30;13:6929-39. doi: 10.2147/IJN.S174909, PMID 30464451
9. Khan AK, Kousar S, Tungmunnithum D, Hano C, Abbasi BH, Anjum S. Nano-elicitation as an effective and emerging strategy for *in vitro* production of industrially important flavonoids. Appl Sci (Basel). 2021 Feb 14;11(4):1694. doi: 10.3390/app11041694
10. Haddadian A, Robattorki FF, Dibah H, Soheili A, Ghanbarzadeh E, Sartipnia N, *et al*. Niosomes-loaded selenium nanoparticles as a new approach for enhanced antibacterial, anti-biofilm, and anticancer activities. Sci Rep. 2022 Dec 19;12(1):21938. doi: 10.1038/s41598-

022-26400-x, PMID 36536030
11. Palani B, Vajjiravelu R, Shanmugam R, Jayakodi S. A comprehensive review of traditional medicinal plants and their role in ovarian cancer treatment. S Afr J Bot. 2025 Jun 1;181:426-45. doi: 10.1016/j.sajb.2025.04.019
12. Puri A, Mohite P, Ansari Y, Mukerjee N, Alharbi HM, Upaganlawar A, *et al*. Plant-derived selenium nanoparticles: Investigating unique morphologies, enhancing therapeutic uses, and leading the way in tailored medical treatments. Mater Adv. 2024;5(9):3602-28. doi: 10.1039/D3MA01126G
13. Vajjiravelu R, Palani B, Shanmugam R, Jayakodi S. Bioinspired nanoparticles mediated from bioactive plants and their therapeutic application in liver cancer. Biomed Mater Devices. 2025 May 21;191:1-6. doi: 10.1007/s44174-025-00361-x
14. Vahdati M, Tohidi Moghadam T. Synthesis and characterization of selenium nanoparticles-lysozyme nanohybrid system with synergistic antibacterial properties. Sci Rep. 2020 Jan 16;10(1):510. doi: 10.1038/s41598-019-57333-7, PMID 31949299
15. Tharani M, Rajeshkumar S, Al-Ghanim KA, Nicoletti M, Sachivkina N, Govindarajan M. *Terminalia chebula*-assisted silver nanoparticles: Biological potential, synthesis, characterization, and ecotoxicity. Biomedicines. 2023 May 18;11(5):1472. doi: 10.3390/biomedicines11051472, PMID 37239143
16. Shahabadi N, Zendehcheshm S, Khademi F. Selenium nanoparticles: Synthesis, *in-vitro* cytotoxicity, antioxidant activity and interaction studies with ct-DNA and HSA, HHb and cyt c serum proteins. Biotechnol Rep (Amst). 2021 Jun;30:e00615. doi: 10.1016/j.btre.2021.e00615, PMID 33948440
17. Bartosiak M, Giersz J, Jankowski K. Analytical monitoring of selenium nanoparticles green synthesis using photochemical vapor generation coupled with MIP-OES and UV-vis spectrophotometry. Microchem J. 2019 Mar;145:1169-75. doi: 10.1016/j.microc.2018.12.024
18. Xu X, Pan Y, Liu X, Han Z, Chen S. Constructing selenium nanoparticles with enhanced storage stability and antioxidant activities via conformational transition of curdlan. Foods. 2023 Jan 27;12(3):563. doi: 10.3390/foods12030563, PMID 36766092
19. Shanmugam R, Munusamy T, Jayakodi S, Al-Ghanim KA, Nicoletti M, Sachivkina N, *et al*. Probiotic-bacteria (*Lactobacillus fermentum)*-wrapped zinc oxide nanoparticles: Biosynthesis, characterization, and antibacterial activity. Fermentation. 2023;9(5):413. doi: 10.3390/fermentation9050413
20. Chen W, Yue L, Jiang Q, Xia W. Effect of chitosan with different molecular weight on the stability, antioxidant and anticancer activities of well-dispersed selenium nanoparticles. IET Nanobiotechnol. 2019 Feb;13(1):30-5. doi: 10.1049/iet-nbt.2018.5052, PMID 30964034
21. Bradley Z, Coleman PA, Courtney MA, Fishlock S, McGrath J, Uniacke-Lowe T, *et al*. Effect of selenium nanoparticle size on IL-6 detection sensitivity in a lateral flow device. ACS Omega. 2023 Mar 7;8(9):8407-14. doi: 10.1021/acsomega.2c07297, PMID 36910974
22. Shanmugam R, Tharani M, Abullais SS, Patil SR, Karobari MI. Black seed assisted synthesis, characterization, free radical scavenging, antimicrobial and anti-inflammatory activity of iron oxide nanoparticles. BMC Complement Med Ther. 2024 Jun 20;24(1):241. doi: 10.1186/s12906-024-04552-9, PMID 38902620
23. Tabibi M, Aghaei S, Amoozegar MA, Nazari R, Zolfaghari MR. Characterization of green synthesized selenium nanoparticles (SeNPs) in two different indigenous halophilic bacteria. BMC Chem. 2023 Sep 16;17(1):115. doi: 10.1186/s13065-023-01034-w, PMID 37716996
24. Chen W, Cheng H, Xia W. Progress in the surface functionalization of selenium nanoparticles and their potential application in cancer therapy. Antioxidants (Basel). 2022 Sep 30;11(10):1965. doi: 10.3390/antiox11101965, PMID 36290687
25. Sans-Serramitjana E, Obreque M, Muñoz F, Zaror C, Mora ML, De Viñas M, *et al*. Antimicrobial activity of selenium nanoparticles (SeNPs) against potentially pathogenic oral microorganisms: A scoping review. Pharmaceutics. 2023 Aug 31;15(9):2253. doi: 10.3390/pharmaceutics15092253, PMID 37765222
26. Filipović N, Ušjak D, Milenković MT, Zheng K, Liverani L, Boccaccini AR, *et al*. Comparative study of the antimicrobial activity of selenium nanoparticles with different surface chemistry and structure. Front Bioeng Biotechnol. 2021 Jan 25;8:624621. doi: 10.3389/fbioe.2020.624621, PMID 33569376
27. Rajeshkumar S, Jayakodi S, Tharani M, Alharbi NS, Thiruvengadam M. Antimicrobial activity of probiotic bacteria-mediated cadmium oxide nanoparticles against fish pathogens. Microb Pathog. 2024 Apr;189:106602. doi: 10.1016/j.micpath.2024.106602, PMID 38408546
28. Cittrarasu V, Kaliannan D, Dharman K, Maluventhen V, Easwaran M, Liu WC, *et al*. Green synthesis of selenium nanoparticles mediated from *Ceropegia bulbosa* Roxb extract and its cytotoxicity, antimicrobial, mosquitocidal and photocatalytic activities. Sci Rep. 2021 Jan 13;11(1):1032. doi: 10.1038/s41598-020-80327-9, PMID 33441811
29. Mekkawy AI, Fathy M, Mohamed HB. Evaluation of different surface coating agents for selenium nanoparticles: Enhanced anti-inflammatory activity and drug loading capacity. Drug Des Devel Ther. 2022 Jun 13;16:1811-25. doi: 10.2147/DDDT.S360344, PMID 35719212
30. Sentkowska A, Konarska J, Szmytke J, Grudniak A. Herbal polyphenols as selenium reducers in the Green synthesis of selenium nanoparticles: Antibacterial and antioxidant capabilities of the obtained SeNPs. Molecules. 2024 Apr 9;29(8):1686. doi: 10.3390/molecules29081686, PMID 38675506
31. Parthasarathy PR, Shanmugam R, Varshan I. *In vitro* anti-diabetic activity of pomegranate peel extract-mediated strontium nanoparticles. Cureus. 2023 Dec 30;15(12):e51356.
32. Yuan Q, Xiao R, Afolabi M, Bomma M, Xiao Z. Evaluation of antibacterial activity of selenium nanoparticles against food-borne pathogens. Microorganisms. 2023 Jun 7;11(6):1519. doi: 10.3390/microorganisms11061519, PMID 37375021
33. Rehman A, John P, Bhatti A. Biogenic selenium nanoparticles: Potential solution to oxidative stress mediated inflammation in rheumatoid arthritis and associated complications. Nanomaterials (Basel). 2021 Aug 5;11(8):2005. doi: 10.3390/nano11082005, PMID 34443836
34. Sasidharan I, Menon AN. Comparative chemical composition and antimicrobial activity fresh & dry ginger oils (*Zingiber officinale* Roscoe). Int J Curr Pharm Res. 2010;2(4):40-3.
35. Rani AP, Archana N, Teja PS, Vikas PM, Sekaran MS. Antimicrobial activity of medicinal plants. Int J Appl Pharm. 2010;2(3):15-21.